11th International Symposium on Turbulence and Shear Flow Phenomena (TSFP11)
Southampton, UK, July 30 to August 2, 2019

A DNS/URANS APPROACH FOR SIMULATING ROUGH-WALL TURBULENT FLOWS

F. Alves Portela
Faculty of Engineering and the Environment
University of Southampton
Southampton SO17 1BJ, UK
f.alves-portela@soton.ac.uk

N. D. Sandham
Faculty of Engineering and the Environment
University of Southampton
Southampton SO17 1BJ, UK
n.sandham@soton.ac.uk

ABSTRACT

An approach targeted at solving high Re_τ rough wall turbulence is developed. This method combines DNS of the roughness layer with RANS models away from the wall by exchanging the Reynolds stresses between the different equations. Computational savings are achieved by making the DNS domain only as large as necessary to resolve the roughness layer. This is the reverse of wall modelled LES, in which a turbulence model is used near the wall. The method is validated on turbulent channel flow simulations up to $Re_\tau = 720$ and applied to the flow over a grit-blasted surface for which DNS results are available.

INTRODUCTION

The effect of roughness in wall-bounded flows is usually modelled by means of an effective roughness height k_s whose relation to a given rough surface can be found by comparing the skin friction of the rough and "clean" configurations (Jiménez, 2004) under fully rough conditions; the added resistance due to the roughness is usually measured in terms of ΔU^+, the difference between the velocities at the centreline of the channel (or top of the boundary layer), considering smooth and rough cases. Alternatively one could also look at the shift in the log laws between the two velocity profiles (rough and smooth). Experimentally, such an approach can be rather cumbersome if one is interested in characterising a broad range of rough surfaces, while the numerical approach is limited either in terms of computationally resolvable Re_τ, in the case of direct numerical simulations (DNS), or by the choice of wall model, in the case of large eddy simulations (LES) or Reynolds averaged Navier-Stokes models (RANS).

At the same time, experiments on boundary layers by Krogstad (1992) show that the presence of roughness elements can lead to mean velocity profiles which cannot be obtained from their rescaled smooth-wall counterparts. This suggests that the flow characteristics in the vicinity of the roughness elements may depend upon details of those elements and cannot be represented by a single parameter k_s.

Given the apparent lack of success in modelling the effect of roughness, Flack (2018) argues that DNS must be incorporated in studies aimed at determining the added skin friction due to realistic surfaces at industry-relevant friction Reynolds numbers Re_τ. A successful DNS resolves the smallest (viscous) scales, of order δ_ν while representing the large coherent structures, which typically scale with δ, imposed through the boundary conditions of the flow (Jiménez *et al.*, 2001). In the case of a turbulent channel flow, δ is the channel's half-height. These structures are essential in maintaining the turbulence regeneration cycle (Tennekes & Lumley, 1972) which means that DNS can quickly become prohibitive since $Re_\tau = \delta/\delta_\nu$.

In the context of LES, a rough-wall can either be treated by a wall-model or by fully resolving the turbulence in its vicinity (Pope, 2000). Wall-models require a certain degree of knowledge about the surface properties (e.g. its parametrisation in terms of k_s) whereas for wall-resolved LES the computational costs scale similarly as in a DNS with increasing Re_τ. Naturally, RANS treatment of rough wall turbulence suffers from the same issues as the aforementioned wall-modelled LES.

Interest in increasing accuracy of flow solutions for industrially relevant Reynolds numbers, not limited to wall turbulence, has pushed for the development of hybrid models in which RANS and LES are used simultaneously in different parts of the flow (Fröhlich & von Terzi, 2008). In wall-bounded turbulence hybrid models usually employ RANS in the vicinity of the wall and "switch" to LES somewhere in the log-layer. As noted by Fröhlich & von Terzi (2008) and by Hamba (2003), a mismatch in velocity profile develops at the interface between the models, independent of blending function or specific LES/RANS models employed. Hamba (2003) bypassed this issue by feeding DNS information to the turbulence models, which is only practical when solving flows for which DNS are available (in which case turbulence-modelled simulations are, arguably, redundant).

As mentioned above, for applications where wall-models cannot be used, the computationally more "afford-

able" tool is wall-resolved LES. This approach has found a mixed degree of success. As argued by Cabot & Moin (2000), the fact that the resolution of wall-resolved LES is usually only increased in the wall normal direction hinders the very idea of obtaining a wall-resolved solution since the turbulence itself may remain unresolved in the remaining spatial directions.

Drawing inspiration from the methods discussed above, we propose a new method for rough surface simulations in which DNS resolution of the wall layer can be achieved at a fraction of the cost of a full-scale DNS of the whole flow. The computational savings are obtained by solving the flow in small domains. In order to prevent the flow from laminarising (or becoming incipiently turbulent), we propose to blend the DNS with a turbulence model. Here unsteady RANS models are used to stabilise the solution in the core of the flow.

In the present paper, we begin by outlining the method itself, which we call a stress-blended method (SBM). We then validate the SBM for low/intermediate Re_τ by carrying out smooth-wall turbulence simulations in domains of different sizes. The method is further assessed in the context of rough wall turbulence using a parametric forcing approach to mimic roughness effects. We show that the mean velocity profiles obtained with the SBM (using roughly an order of magnitude fewer points than a full scale DNS) are close to those obtained by DNS. Finally we test SBM on a scanned grit-blasted surface and outline limitations and further developments and applications of the method.

THE STRESS-BLENDED METHOD

Our goal is to blend the model-free (incompressible) Navier-Stokes equations

$$\frac{\partial u_i}{\partial t}+\frac{\partial u_i u_j}{\partial x_j}=-\frac{\partial p}{\partial x_i}+\nu\frac{\partial^2 u_i}{\partial x_j \partial x_j}+G_i, \qquad (1)$$

which are solved in a traditional DNS, with the unsteady RANS equation. In the context of turbulent channel flow, the latter reads

$$\frac{\partial U}{\partial t}+\frac{\partial}{\partial x_3}\left(\nu_t\frac{\partial U}{\partial x_3}\right)=\nu\frac{\partial^2 U}{\partial x_3^2}+G_1, \qquad (2)$$

where the spatial coordinates are defined as in fig. 1.

In eqs. (1) and (2) G_i is the driving force which sets the friction Reynolds number ($G_i=0$ for $i=2,3$), $u_i=u_i(x_i,t)$ is the instantaneous fluid velocity, $p=p(x_i,t)$ is the pressure divided by density and ν is the fluid's kinematic viscosity, $U=U(x_3,t)$ is an unsteady mean velocity and ν_t is the turbulent eddy viscosity obtained by means of some RANS model.

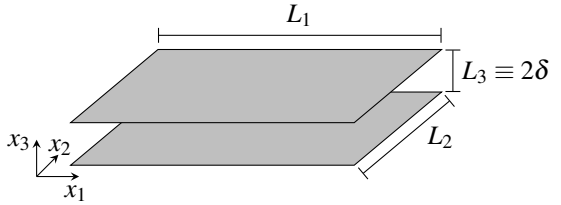

Figure 1: Channel dimensions and coordinate system. δ is the half-channel height.

Formulation and governing equations

The first challenge in exchanging information between eq. (1) and eq. (2) is that fields associated with the RANS must involve an averaging procedure. We define mean quantities as

$$U_i=\langle u_i\rangle=\iint u_i \mathrm{d}x_1 \mathrm{d}x_2, \qquad (3)$$

which are simply averages in the homogeneous spatial directions of the channel (x_1,x_2 as illustrated in fig. 1).

In order to construct an equation that blends eq. (1) and eq. (2), we need to introduce a blending coefficient $\beta=\beta(x_3)$. We set $\beta=0$ in regions where the RANS model is not to be used and $\beta=1$ for the reverse situation whereas regions $0<\beta<1$ are deemed as the blending interface. As will be seen below, within the interface β can take any functional form, provided that necessary corrections are applied to the governing equations.

Recalling eq. (3) and using β defined above, we are now in a position to blend the DNS and RANS equations. Taking the mean of eq. (1) multiplied by β and adding it to eq. (2) multiplied by $1-\beta$ yields

$$\frac{\partial U}{\partial t}+(1-\beta)\langle\frac{\partial u_1 u_3}{\partial x_3}\rangle-\beta\frac{\partial}{\partial x_3}\left(\nu_t\frac{\partial U}{\partial x_3}\right) =\nu\frac{\partial^2 U}{\partial x_3 \partial x_3}+G_1. \qquad (4)$$

Equation (4) is thus a governing equation for the mean velocity which takes in the Reynolds stresses from either the DNS or a RANS model, depending on the region of the flow, i.e. the turbulence modelling is restricted to regions where $\beta=1$. Since eq. (4) is an equation for $\langle u_1\rangle$, an equation for u_1 that includes information from the RANS reads

$$\frac{\partial u_1}{\partial t}+\frac{\partial u_1 u_j}{\partial x_j}-\beta\left[\langle\frac{\partial u_1 u_3}{\partial x_3}\rangle+\frac{\partial}{\partial x_3}\left(\nu_t\frac{\partial U}{\partial x_3}\right)\right] =-\frac{\partial p}{\partial x_1}+\nu\frac{\partial^2 u_1}{\partial x_j \partial x_j}+G_1, \qquad (5)$$

while the equations for u_2 and u_3 remain unchanged.

Equation (5) thus represent a stress-blended DNS RANS equation since the difference to eq. (1) is the addition of $-\beta\left[\langle\frac{\partial u_1 u_3}{\partial x_3}\rangle+\frac{\partial}{\partial x_3}\left(\nu_t\frac{\partial U}{\partial x_3}\right)\right]$ which effectively sets the mean Reynolds stresses to either those arising directly in the flow or those obtained by means of a RANS model, which is desirable in circumstances where the turbulence may become incipient or close to laminarisation.

DNS/RANS interface

While eq. (5) reduces to either eq. (1) or eq. (2), depending on whether $\beta=0$ or $\beta=1$, it yields neither at the interface. This issue arises due to the fact that $\langle\frac{\partial u_1 u_3}{\partial x_3}\rangle$ is unlikely to be exactly equal to its RANS counterpart, $-\frac{\partial}{\partial x_3}\left(\nu_t\frac{\partial U}{\partial x_3}\right)$. The bulk difference between those two

quantities across the interface results in a net driving force, which in turn affects the shear stress at the wall.

This effect can be seen by carrying out a global momentum balance within the channel. Integrating eq. (5) over the whole domain (or equivalently, integrating eq. (4) between the two walls) yields

$$\int_0^{2\delta} \frac{\partial U}{\partial t} \mathrm{d}x_3 - \int_0^{2\delta} \beta \left[\langle \frac{\partial u_1 u_3}{\partial x_3} \rangle + \frac{\partial}{\partial x_3} \left(\nu_t \frac{\partial U}{\partial x_3} \right) \right] \mathrm{d}x_3 = \nu \frac{\partial U}{\partial x_3}|_{x_3=2\delta} - \nu \frac{\partial U}{\partial x_3}|_{x_3=0} + G_1 2\delta. \quad (6)$$

Using the chain rule the second integral in the equation above can be re-written as

$$- \int_0^{2\delta} \frac{\partial \beta}{\partial x_3} \left(\langle u_1 u_3 \rangle + \nu_t \frac{\partial U}{\partial x_3} \right) \mathrm{d}x_3, \quad (7)$$

whose integrand is non-zero only at the interface, where $\frac{\partial \beta}{\partial x_3} \neq 0$.

Defining $x_3^{\beta 1}$ and $x_3^{\beta 2}$ as the interface bounds[1], taking the time average (indicated by $\overline{\cdot}$) of eq. (6) eliminates the transient term and by further making use of the channel's symmetry eq. (6) becomes

$$- \int_{x_3^{\beta 1}}^{x_3^{\beta 2}} \frac{\partial \beta}{\partial x_3} \left(\langle \overline{u_1 u_3} \rangle + \overline{\nu_t \frac{\partial U}{\partial x_3}} \right) \mathrm{d}x_3 = -\nu \frac{\partial \overline{U}}{\partial x_3}|_{x_3=0} + G_1 \delta. \quad (8)$$

The driving force G_1 is normally chosen such that it balances out the right hand side of eq. (8), yielding u_τ^2/δ (where u_τ is the friction velocity). The approach here is to make $G_1 = G_1(t)$ and set it to $u_\tau^2 \delta$ minus the contribution due to the SBM, given by eq. (7). Notice that in the case where the interface is sharp ($x_3^{\beta 1} = x_3^{\beta 2}$) eq. (7) gives the exact difference between the DNS and RANS Reynolds stresses at the interface. Simulations for smooth wall turbulence at $Re_\tau = 180$ with different interface shapes and locations revealed little sensitivity to those variations in the interface; as such, all the results that follow were obtained with sharp interfaces located at 60 wall units from the walls.

NUMERICAL METHOD

The simulations have been carried out using second-order accurate finite-differences on a staggered grid for the spatial discretisation and a second-order accurate Adams-Bashforth method for the time integration. The domain sizes and grid points used can be found in table 1. The grid is stretched in the wall normal direction using a hyperbolic tangent, with the smallest grid spacing being δ_ν and the largest being $4\delta_\nu$. From table 1 cases A and C represent typical domains/grids used in full scale DNS; furthermore, cases B, D and G represent domain sizes approaching the so called minimal flow unit (Jiménez & Moin, 1991).

[1] In the case of channel a second interface exists bounded at $2\delta - x_3^{\beta 2}$ and $2\delta - x_3^{\beta 1}$.

Case	Re_τ	$[L_1, L_2, L_3]/\delta$	$[N_1, N_2, N_3]$
A	180	$[2\pi, \pi, 2]$	$[128, 128, 128]$
B	180	$[\pi, \pi/2, 2]$	$[64, 64, 128]$
C	360	$[2\pi, \pi, 2]$	$[256, 256, 256]$
D	360	$[\pi, \pi/2, 2]$	$[128, 128, 256]$
E	360	$[\pi/2, \pi/4, 2]$	$[64, 64, 256]$
F	720	$[\pi/2, \pi/4, 2]$	$[128, 128, 512]$
G	720	$[\pi/4, \pi/8, 2]$	$[64, 64, 512]$

Table 1: Domain sizes and resolution used for smooth wall and parametric forcing simulations.

In addition to the smooth and parametric forcing simulations, the SBM was also tested by simulating the flow over a grit-blasted surface. The chosen surface has been extensively studied by Busse *et al.* (2017) by means of DNS and is thus an ideal test case for assessing the performance of the SBM on realistic flows. The no-slip boundary condition is imposed by iterative application of an immersed boundary method introduced in Busse *et al.* (2015).

Parametric forcing

In validating the SBM the effect of roughness was firstly introduced using the parametric forcing approach developed by Busse & Sandham (2012). There, a source term is added to eq. (1) of the form

$$- \alpha_i F_i(x_3, h) u_i |u_i|, \quad (9)$$

without summing over repeated indices and where α_i represents the magnitude of the force, F_i is a shape-function which depends on the wall-normal distance (x_3) and the roughness height h. In the present contribution, the coefficients α_i were all set to 1 and a box profile was used for F_i.

In the present work eq. (9) is useful in assessing the performance of the SBM as it provides a simple framework for varying k^+ and thus obtaining ΔU^+ vs k^+ curves for the different configurations listed in table 1. Furthermore, in the context of validating the SBM, the parametric forcing approach removes complications associated with choosing representative portions of scanned surfaces.

As will be seen below, RANS simulations were carried out in support of the SBM approach. Due to the nature of RANS, only the contribution of the mean velocity to eq. (9) (i.e. $-\alpha F(x_3, h)\overline{U}|\overline{U}|$) was used. While Forooghi *et al.* (2018) have shown that the neglected contribution is in some cases smaller than $-\alpha F(x_3, h)\overline{U}|\overline{U}|$, this issue only persists for RANS simulations, since, in SBM the full (mean and fluctuating) velocity component is available.

RANS models

Two RANS models have been assessed, which are known to provide reasonably accurate results for turbulent channel flow: the algebraic mixing length model (ML) using the van Driest damping function (*cf.* pp. 302, 366-368 in Pope, 2000) and the one-equation model by Spalart

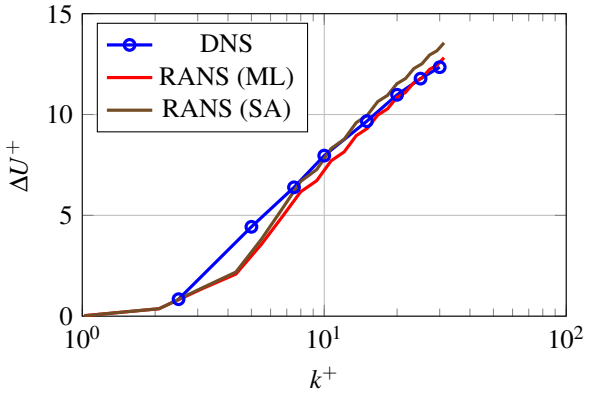

Figure 2: Centreline velocity deficit obtained with full scale DNS and RANS at $Re_\tau = 180$ with parametric forcing.

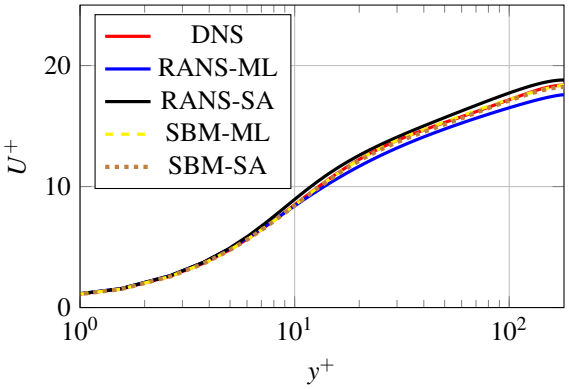

Figure 3: Mean velocity profiles for configuration A (see table 1).

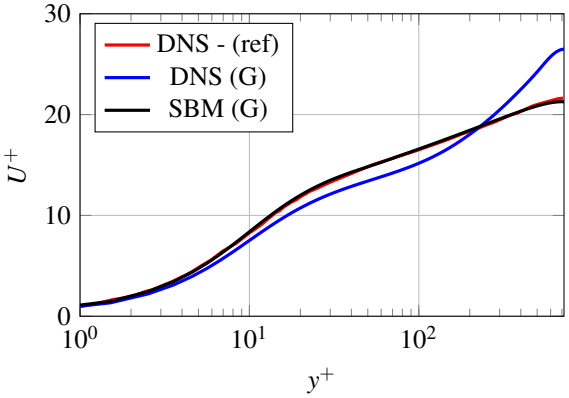

Figure 4: Mean velocity profiles for smooth wall turbulence at $Re_\tau = 720$ (see table 1). The DNS - (ref) profile was extracted from Hu *et al.* (2006) and corresponds to a full scale DNS.

& Allmaras (1992) usually referred to as Spalart Almaras model (SA). Notice that the SBM is not limited to these two models and can, in principle, be used with any RANS model.

Independent RANS simulations using the parametric forcing approach described above yielded ΔU^+ vs k^+ curves reasonably close to those obtained by full scale DNS, as shown in fig. 2. This provides some confidence that RANS is useful for the roughness problem, provided it has a realistic wall friction value. As seen in that figure, both models are practically indistinguishable in the hydrodynamically smooth range of k^+ and are fairly close to the DNS. At higher k^+ the curves corresponding to the RANS simulations display a higher slope than those corresponding to the DNS, this is likely due to the missing contribution from the turbulent fluctuations. Furthermore, both models seem to enter the transitionally rough regime at slightly different values of k^+, with SA appearing to be closer to the DNS for $k^+ \sim 10$ than ML.

RESULTS

As a validation step, we first compare the accuracy of SBM with regards to DNS and RANS in smooth wall turbulence. Further simulations were carried out as shown in table 1 with domain sizes substantially smaller than those required for a full scale DNS. These simulations were of both smooth wall turbulence as well as using the parametric forcing approach described above. Finally as simulation of the flow over a grit-blasted surface was carried out, spanning $Re_\tau = 180, 360, 720$ and keeping the domain size constant in terms of wall units.

Smooth wall

First, the SBM simulations of case A (which corresponds to a full scale DNS configuration) were carried out and compared to the corresponding DNS and RANS (using the same grid). The resulting mean velocity profiles are shown in fig. 3 as well as mean velocity profiles obtained from independent RANS simulations.

Figure 3 shows that, the SBM yields almost the same solution as the DNS. Recall that fig. 3 corresponds to the full scale configuration (case A). Nevertheless, this figure illustrates that the introduction of the blending of the RANS with the DNS has little effect on the statistics of the flow and yields better results than independent RANS (admittedly, at the same cost as the DNS) in this case. Simulations were also carried out for case B, where statistics from both the DNS and SBM showed no significant differences with respect to case A and therefore are not included here. Figure 3 shows no difference between the SBM simulations using either of the RANS models. For the remainder of this paper the Spalart-Allmaras model is used since it proved to be more robust for small-domain cases.

It should be noted that the dimensions of case B are quite close to the minimal channel dimensions proposed by Jiménez & Moin (1991). As such, shrinking the domain size beyond that of case B leads to laminarisation. For higher Re_τ, however, where the turbulence sustains, the reduction of domain led to an increase of the velocity profile in the wake region of the DNS. Figure 4 makes this issue very evident. In that figure, the mean velocity profile obtained with the DNS in configuration G barely displays a log-law, contrary to that obtained with the SBM which falls very closely onto the DNS curve extracted from Hu *et al.* (2006).

Parametric forcing

Further simulations were carried out using the parametric forcing approach of Busse & Sandham (2012). The different coefficients were set to $\alpha_i = 1$ and F_i was set to a top hat profile such that $F_i = 1, y^+ < 2k^+$.

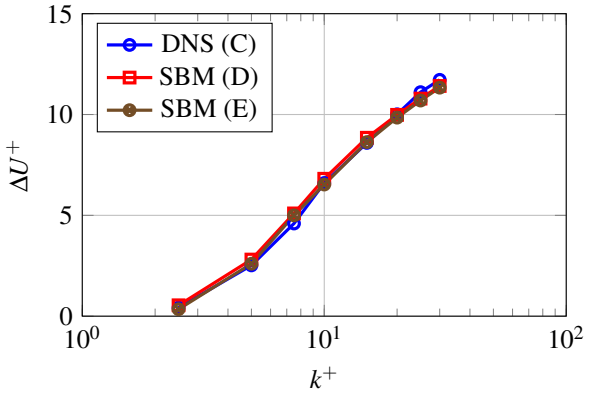

Figure 5: ΔU^+ vs k^+ using parametric forcing for cases C, D and E.

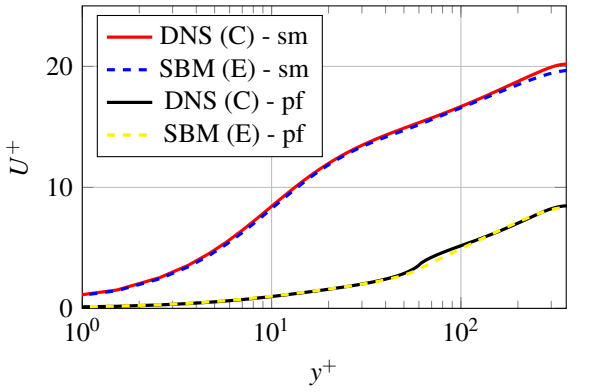

Figure 6: Comparison of mean velocity profiles between cases C and E, using DNS and SBM respectively. The different pairs of curves correspond to smooth wall (sm) and parametric forcing (pf).

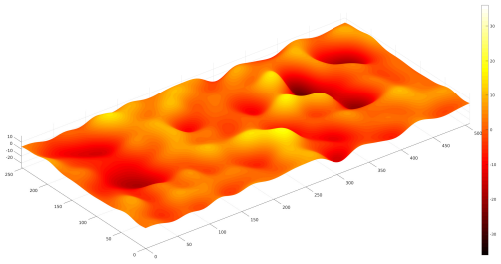

Figure 7: Illustration of the grit blasted surface used. All dimensions are in wall units.

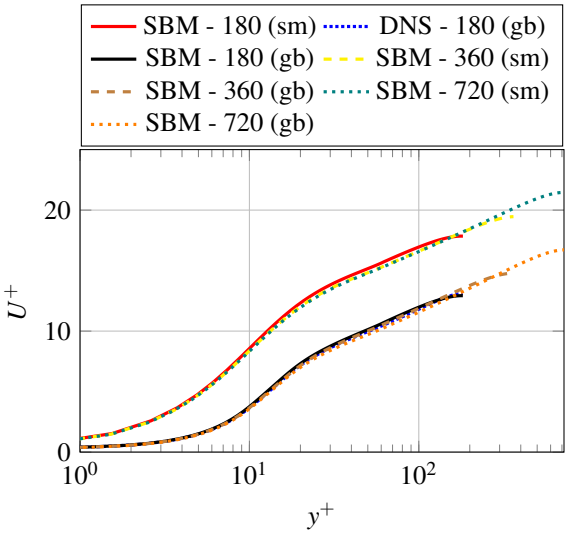

Figure 8: Mean velocity profiles of flow over a grit-blasted surface (gb) and smooth wall (sm).

For reference, full-scale DNS simulations were carried out for the $Re_\tau = 180$ and $Re_\tau = 360$ cases (i.e. A and C in table 1). Figure 5 shows the variation of ΔU^+ with k^+ obtained with the SBM and compared to the full-scale DNS at $Re_\tau = 360$. An excellent match between SBM and DNS values of ΔU^+ can be observed in that figure. Notice from fig. 5 that, even when the flow domain is shrunk by a factor 4, in the stream- and span-wise directions, the SBM yields near DNS values of ΔU^+. This is also illustrated in fig. 6 where the velocity profiles obtained with the SBM in small domains are very close to those obtained by DNS in large domains. The values of ΔU^+ obtained for cases F and G also showed no significant dependence on the domain size when using SBM.

Flow over a grit blasted surface

Finally, the SBM was employed in solving the flow over a scanned surface. A grit-blasted surface from Thakkar (2017) was chosen. The SBM simulations were carried out on a sample smaller (by a factor of 4 in area) than that used in the full-scale DNS of Thakkar (2017) which is illustrated in fig. 7; Thakkar (2017) studied the same small surface sample at $Re_\tau = 180$. The surface has a skewness of -0.6, flatness of 3.8 and a maximum peak to valley k^+_{pv} of 44.5. The simulations were carried out at $Re_\tau = 180$, $Re_\tau = 360$ and $Re_\tau = 720$ with constant $k^+ = 23$, obtained by taking the mean of the maximum peak to valley heights of equally sized subsamples (after splitting the surface into 5 by 5 sections). The stream- and span-wise domain sizes L_1^+ and L_2^+ (recall fig. 1) were set to 506.7 and 253.35, respectively.

The SBM employed the Spalart-Allmaras model and eq. (6) was modified such that the integration bounds are those of the simulation (rather than the distance between the surfaces).

Figure 8 compares the mean velocity profiles obtained with the SBM and the DNS results of Thakkar (2017) at $Re_\tau = 180$ as well as the profiles obtained by SBM for $Re_\tau = 360$ and $Re_\tau = 720$. For the case where DNS data is available, excellent agreement between the DNS and the SBM.

Table 2 summarises the data shown in fig. 8 in terms of ΔU^+ and flow configurations. Since k^+ is kept constant, one would expect ΔU^+ to remain constant with varying Reynolds number. The small variations in ΔU^+ between the different Re_τ can thus be attributed to the variation in blockage, which was also observed in the blockage study of Thakkar (2017). The results indicate that errors of less than 4% in ΔU^+ are incurred isomg a blockage factor up to $k/\delta = 0.13$.

At $Re_\tau = 180$, the centreline velocity deficit ΔU^+ obtained with the SBM was of 4.93, below the value of 5.33 reported by Thakkar (2017). In fact, it should be noted that reference smooth velocity used by Thakkar (2017) was not

Re_τ	U_c^+	ΔU^+	L_1/δ	L_2/δ	k^+	k/δ
180	12.93	4.93	2.8	1.4	23	0.13
360	14.78	4.80	1.4	0.7	23	0.06
720	16.60	4.76	0.7	0.35	23	0.03

Table 2: Flow configurations and corresponding ΔU^+ for grit-blasted simulations.

obtained in such a small domain (but rather from configuration A), if the same reference is used here, the value of ΔU^+ for $Re_\tau = 180$ obtained with the SBM is actually 5.26.

CONCLUSION

A novel hybrid method for tackling wall-bounded turbulent flows, called stress-blended method (SBM), has been presented. The method relies on exchanging the Reynolds stresses between the DNS and RANS regions over an interface.

Preliminary tests show that the shape and size of the interface have little effect on the flow, so long as it lies within the log-layer. The mismatch between the DNS and RANS stresses over the interface requires special considerations with regards to the overall momentum balance as it results in an artificial driving of the flow. The present approach does not appear to suffer from the same interface issues of other RANS/LES hybrid methods (Fröhlich & von Terzi, 2008).

When the SBM was employed in full-scale simulations the resulting mean velocity profiles are almost the same as those obtained with DNS. As predicted by Jiménez & Moin (1991), shrinking of the domain results in laminarisation of the flow near the core of the channel, which manifests itself in the increased wakes obtained by DNS. However, for flows computed through SBM, no such increase in the wake profiles was observed and, in fact, the mean velocity profiles were found to be close to the full-scale DNS profiles.

The performance of SBM in the presence of roughness is validated by means of the parametric forcing approach of Busse & Sandham (2012). We find that the SBM is able to accurately predict the added resistance in domains up to 8 times smaller (in the stream- and span-wise directions) than a full-scale DNS would require. In such cases, the computational costs is effectively 1/64 of the DNS. Similarly positive results were obtained by applying the SBM to simulations over a grit-blasted surface.

ACKNOWLEDGEMENTS

The authors acknowledge the support of EPSRC through the grant number EP/P009638/1.

REFERENCES

Busse, A., Lützner, M. & Sandham, N. D. 2015 Direct numerical simulation of turbulent flow over a rough surface based on a surface scan. *Computers & Fluids* **116**, 129 – 147.

Busse, A. & Sandham, N. D. 2012 Parametric forcing approach to rough-wall turbulent channel flow. *Journal of Fluid Mechanics* **712**, 169–202.

Busse, A., Thakkar, M. & Sandham, N. D. 2017 Reynolds-number dependence of the near-wall flow over irregular rough surfaces. *Journal of Fluid Mechanics* **810**, 196–224.

Cabot, W. & Moin, P. 2000 Approximate wall boundary conditions in the large-eddy simulation of high reynolds number flow. *Flow, Turbulence and Combustion* **63** (1), 269–291.

Flack, K. A. 2018 Moving beyond Moody. *Journal of Fluid Mechanics* **842**, 1–4.

Forooghi, P., Frohnapfel, B., Magagnato, F. & Busse, A. 2018 A modified Parametric Forcing Approach for modelling of roughness. *International Journal of Heat and Fluid Flow* **71** (March), 200–209.

Fröhlich, J. & von Terzi, D. 2008 Hybrid les/rans methods for the simulation of turbulent flows. *Progress in Aerospace Sciences* **44** (5), 349 – 377.

Hamba, F. 2003 A hybrid rans/les simulation of turbulent channel flow. *Theoretical and Computational Fluid Dynamics* **16** (5), 387–403.

Hu, Z., Morfey, C. L. & Sandham, N. D. 2006 Wall pressure and shear stress spectra from direct simulations of channel flow. *AIAA Journal* **44** (7), 1541–1549.

Jiménez, J. 2004 Turbulent flows over rough walls. *Annual Review of Fluid Mechanics* **36** (1), 173–196.

Jiménez, J., Flores, O. & García–Villalba, M. 2001 The large-scale organization of autonomous turbulent wall regions. *Tech. Rep.*. Center for Turbulence Research.

Jiménez, J. & Moin, P. 1991 The minimal flow unit in near-wall turbulence. *Journal of Fluid Mechanics* **225**, 213–240.

Krogstad, P-Å. 1992 Comparison between rough-and smooth-wall turbulent boundary layers. *Journal of Fluid Mechanics* **245**, 599–617.

Pope, S. B. 2000 *Turbulent Flows*. Cambridge University Press.

Spalart, P. R. & Allmaras, S. R. 1992 A one-equation turbulence model for aerodynamic flows. In *30th aerospace sciences meeting and exhibit*, p. 439.

Tennekes, H. & Lumley, J. L. 1972 *A First Course in Turbulence*. MIT Press.

Thakkar, M. 2017 Investigation of turbulent flow over irregular rough surfaces using direct numerical simulations. PhD thesis, University of Southampton.